LRP 717/01 January 2002

Extension of the TCV Operating Space Towards Higher Elongation and Higher Normalized Current

F. Hofmann, S. Coda, P. Lavanchy, X. Llobet,
Ph. Marmillod, Y. Martin, A. Martynov,
J. Mlynar, J.-M. Moret, A. Pochelon,
O. Sauter

Accepted for Publication
in NUCLEAR FUSION

ISSN 0458-5895

Extension of the TCV Operating Space Towards Higher Elongation and Higher Normalized Current

F. Hofmann, S. Coda, P. Lavanchy, X. Llobet, Ph. Marmillod, Y. Martin, A. Martynov, J. Mlynar, J.-M. Moret, A. Pochelon, O. Sauter

Centre de Recherches en Physique des Plasmas,
Association EURATOM - Confédération Suisse,
Ecole Polytechnique Fédérale de Lausanne, CH-1015 Lausanne, Switzerland

Abstract

Recently, an experimental campaign has been launched on TCV with the aim of exploring and extending the limits of the operating space. The vertical position control system has been optimized, with the help of extensive model calculations, in order to allow operation at the lowest possible stability margin. In addition, the growth rate of the axisymmetric instability has been minimized by choosing optimum values for the plasma triangularity and squareness and by operating close to the current limit imposed by the n=1 external kink mode. These measures have allowed us to reach record values of elongation, κ=2.8, and normalized current, I_N=3.6, in a tokamak with standard aspect ratio, R/a=3.5.

1. Introduction

The advantages of elongated and shaped plasma cross-sections are well known and have been demonstrated in several tokamaks [1-4]. For a given safety factor, the plasma current increases with elongation, $I_P \sim (\kappa^2+1)/2$, and according to Troyon scaling [5], the maximum beta value is proportional to the normalized current, $I_N=I_P/(a*B)$. MHD stability calculations [6-8] have shown that the beta limit indeed increases with elongation, in rough agreement with Troyon scaling, but only up to a certain value of κ. Beyond that value, the beta limit stays constant or decreases. The elongation at which the beta limit reaches its maximum depends on a number of parameters, such as the current profile, triangularity, squareness, aspect ratio, etc. In tokamaks with conventional aspect ratio, $3<R/a<4$, this optimum elongation is between 2.2 and 2.4 [6]. In low-aspect-ratio tokamaks, the elongation which maximizes beta is considerably larger [9]. It should be noted, however, that very large tokamaks, such as ITER, are constrained to operate at relatively low elongation, as a result of the large mechanical forces which arise during vertical displacement events and disruptions.

The study of highly elongated plasmas and the experimental investigation of MHD stability limits at high elongation is one of the main aims of TCV. In Ohmic plasmas, i.e. plasmas without localized heating or current profile tailoring, axisymmetric stability imposes a lower limit to the normalized plasma current, and simultaneously, the non-axisymmetric modes impose an upper limit to the current. The stable operating window between these two limits becomes smaller as the elongation increases [8]. In a given tokamak, axisymmetric stability can be improved in several different ways. First, the passive stability can be improved by adapting the plasma shape as closely as possible to the shape of the vacuum vessel. Second, the vertical position control system can be optimized such that operation at very low stability margins becomes possible. Third, the current profile can be widened either by operating at the maximum possible plasma current or by applying localized Electron Cyclotron Heating or Current Drive [10]. Non-axisymmetric stability, on the other hand, can be improved by operating at low beta or at low current, since at high elongation, the current limit increases as beta decreases [11].

In this paper, we describe how the methods for improving plasma stability, as mentioned above, were implemented in TCV and we show that this has led to a considerable extension of the accessible operating space.

2. Optimization of the vertical position control system

The vertical position control system of the TCV tokamak uses active feedback coils both outside and inside the vacuum vessel [12]. The external coils are driven by slow power supplies with a response time of ~1ms. They are used for proportional and derivative feedback. The internal coils are driven by a fast supply with a response time of less than 0.1ms and are used for derivative feedback only. The TCV control system is somewhat similar to the one used on DIII-D, with the exception that DIII-D uses inboard poloidal field coils, rather than coils inside the vacuum vessel, for fast derivative feedback [13].

Closed-loop, axisymmetric stability of the complete system depends on a large number of parameters, such as the properties of the vertical position observer, the signal processing electronics, the PID gains, the power supply characteristics, the location of active coils, the geometry and electrical resistivity of the passive stabilizers and finally, the plasma parameters (shape, current distribution, plasma-wall distance). In order to reach the maximum possible elongation or, equivalently, the minimum stability margin, all of the above parameters must be optimized. This cannot be done experimentally, by trial-and-error methods, since the number of parameters to be varied is much too large. For TCV, we use a numerical model [14], the Deformable Plasma Model (DPM), to optimize the important parameters. This model has been shown to give good agreement with experimental results [15].

Here, we use the DPM to determine the stability properties of the vertical position control system, as a function of the three gain settings, i.e. the proportional and derivative gains (P and D) in the slow feedback loop, feeding the external coils, and the derivative gain (G) in the fast loop acting on the internal coils. As an example, we show the stable domain in three-dimensional gain space, predicted by the DPM for a typical TCV plasma (Fig.1). For each value of the fast derivative gain, G, there is a tear-drop shaped stable island in the plane of the slow gains, P and D. The size of the stable island increases with the fast gain, G, but when G exceeds a critical value (G=74 μs in Fig.1), stability is lost. As a consequence, the cone shaped stable domain is cut off abruptly at G=74μs. The reason for the abrupt cutoff is an instability in the fast control loop, caused by a limited bandwidth and, consequently, a large phase shift at high frequency. This will be discussed below in more detail. The volume of the stable domain, for a given plasma, can be considered as a measure of the overall performance of the control system. We have calculated the stable domain as a function of those system parameters that can actually be varied in the experiment, i.e. the observer characteristics, the transfer functions

and the configuration of the external active coils. The main results of these calculations are summarized in the paragraphs below.

The standard vertical position observer which is used in the fast active loop consists of a linear combination of magnetic probe signals [12]. Varying the coefficients by which the probe signals are multiplied does not lead to significant gains in the stable volume in gain space, with one notable exception. Some of the B-probes are located very close to the internal active coil (probes #14 and #26 in Fig.2) and, in the past, it was thought that the coefficients of these probes had to be zero to avoid direct coupling between the active coil and the observer. However, DPM simulations have shown that it can be advantageous to use non-zero coefficients for the probes in the vicinity of the active coil. If the sign of these coefficients is chosen correctly, the effect is equivalent to a reduction of the self-induction of the internal coil and hence it allows a faster response of the coil current to a given voltage signal.

The overall transfer function of the fast control loop determines the fundamental resonance frequency at which the total phase shift reaches 180^{o}. The choice of this frequency reflects a compromise between noise sensitivity on the one hand and fast response on the other hand. Originally [16], the resonance frequency was chosen to be 2.5kHz, but DPM calculations have shown that the stable volume in gain space can be increased by increasing this frequency to 3.5kHz without unduly aggravating the problems of noise propagation. This modification is equivalent to increasing the bandwidth of the feedback loop. The maximum allowable gain is defined by the condition that the overall loop gain at the resonance frequency must be less than unity, which corresponds to G=74 μs in the example of Fig.1.

In TCV, any combination of external shaping coils can, in principle, be used for vertical position control. DPM calculations have confirmed earlier results [17] indicating that there is an optimum vertical distance between the positive and negative feedback currents. If the two currents are too far apart, global modes of the vacuum vessel are excited and the penetration time of the control fields becomes large. If, on the other hand, the currents are too close together, the magnetic fields cancel each other partially and the coils become inefficient. For highly elongated plasmas in TCV, whose magnetic axis lies slightly above the midplane ($0.05m<Z_{Axis}<0.10m$), the best choice for slow active feedback is to use two pairs of external shaping coils, i.e. [F3, F4] and [F6, F7] (see Fig.2), where the feedback voltages applied to the two coils within each pair are identical and the voltages applied to coils in different pairs are opposite.

3. Plasma shape optimization

3.1. Plasma-wall distance

In TCV, the main passive stabilizing element is the vacuum vessel. The vessel has a rectangular shape (Fig.2) and, ideally, the plasma should have the same shape in order to achieve the maximum stabilizing effect with respect to axisymmetric modes. This is not entirely feasible in TCV, but as a guiding principle, we assume that the average plasma-wall distance should be minimized. This implies, in the case of limiter configurations, that the inboard boundary of the plasma cross-section should be a straight line, and that indented equilibria should be avoided. In addition, the outermost point of the plasma boundary should be as close as possible to the outboard tile surface. This last condition is a consquence of the fact that in TCV, the elongation of the vacuum vessel, as defined by the surface of the carbon tiles (κ=2.9), is larger than the maximum plasma elongation. In other tokamaks, where the vessel elongation is less than the maximum plasma elongation, this condition does, of course, not apply. Originally, TCV had a toroidal belt limiter, installed on the outboard side of the vessel. The belt limiter was removed in 1998 and this allowed us to increase the plasma major and minor radii by 1.2cm. The effect of this modification is a significant reduction of the n=0 growth rate for a given plasma shape and normalized current. For example, at κ=2.5, I_N=2.9, the growth rate is reduced from 3190 s^{-1} to 2380 s^{-1}. It should be noted, however, that reducing the plasma-wall distance does not always improve vertical stability. There are cases where the opposite is true, as will be discussed in section 3.2, below.

3.2. Variation of triangularity and squareness

The shape of the plasma boundary in TCV can be approximately described by the expressions $R = R_0+a\,[\cos(\theta + \delta\sin\theta - \lambda\sin2\theta)]$, $Z = Z_0+a\,\kappa\,\sin\theta$, where R_0 and a are the major and minor radii, respectively, Z_0 measures the vertical position of the magnetic axis, and κ, δ and λ designate elongation, triangularity and squareness, respectively. It is well known that both the n=1 external kink stability and the n=0 axisymmetric stability, at a given elongation, depend on triangularity and squareness [8]. In order to find the best combination of δ and λ, at a fixed elongation, we have performed n=0 and n=1 stability calculations using the DPM [14] and KINX [18] codes. The DPM model gives us the n=0 growth rate in presence of all passive conductors in TCV and KINX is used to calculate the current limit for a given plasma shape and current profile. As a starting point, we use a reconstructed experimental TCV equilibrium with κ=2.70. We then vary triangularity and squareness and, for each combination (δ,

λ), we increase the total current, leaving the profile shape unchanged, until we reach the n=1 stability limit. The reason for increasing the current to its limit is that, in Ohmic plasmas, the internal inductance and, consequently, the n=0 growth rate decrease with increasing current. We find that the current limit increases with δ but decreases with λ (Fig.3A), in agreement with earlier results [8]. The n=0 growth rate is then computed with the DPM model for those plasmas which are close to the n=1 stability limit, as a function of δ and λ (Fig.3B). We note that the n=0 growth rate has a minimum for $\delta \sim 0.6$ and $\lambda \sim 0.25$ and conclude that this corresponds to the optimum choice of the shape parameters. The minimum in γ is relatively shallow, indicating that small variations in δ and λ do not change the growth rate by a large amount. It is important to note that the optimum shape parameters do not coincide with the minimum overall pasma-wall distance. The shape of the vacuum vessel corresponds, approximately, to δ=0, λ=0.7, and the plasma-wall distance would be minimized if the plasma had the same shape parameters. The fact that the minimum axisymmetric growth rate is obtained for much lower values of λ (Fig.3B) is a consequence of the decrease of the current limit with increasing λ (Fig.3A). This implies, in Ohmic plasmas, a peaking of the current profile and, consequently, an increase of the n=0 growth rate, inspite of a decreasing plasma-wall distance.

The theoretical results presented in Fig.3 have been confirmed experimentally. In fact, virtually all experiments at high elongation, $\kappa > 2.5$, were performed with triangularities in the range $0.50 < \delta < 0.63$ and squareness, $0.22 < \lambda < 0.26$. Experimental variations of δ and λ outside these domains have not produced any significant improvement in n=0 stability. It should be noted that the optimum plasma shape, as it is defined here, depends, to a large extent, on the shape of the conducting shell which serves as a passive stabilizer. In TCV, relatively high values of λ are necessary for good n=0 stability because the shape of the passive stabilizer, i.e. the vacuum vessel, is rectangular. In other tokamaks with D-shaped vacuum vessels the optimum plasma shape is characterized by lower values of λ and higher values of δ [4].

Vertical stability of elongated plasmas can also be discused in terms of the "decay index",

$$n = -\left(\frac{R}{B_Z}\right)\left(\frac{\partial B_Z}{\partial R}\right)$$

which measures the local curvature of the poloidal vacuum field [13]. However, in a highly elongated equilibrium, the decay index varies typically by a factor of 4 between the inboard and outboard edges of the plasma, and it can even change sign within the plasma volume. Consequently, it is not obvious which value of n should be used to characterize the system and to

measure the driving force of the instability. Using the value of n on the magnetic axis is somewhat arbitrary and does not reflect the global character of the instability. For this reason, we prefer to use the open loop growth rate, rather than the decay index, to characterize the instability and to optimize the system. The dependence of the open loop growth rate on elongation, triangularity and internal inductance has been discussed previously [14].

3.3. New plasma shapes

The classical shape parameters, κ, δ and λ, do not exhaust the possibilities for shape variation in TCV. Several alternative shapes, some of which are shown in Fig.4, are theoretically possible. We have calculated n=0 and n=1 stabilty properties of these equilibria and, in Table 1, we compare ideal MHD current limits and n=0 growth rates, at the current limit,

Table 1: Parameters of various plasma shapes

	D-shape	Trapezoid	Peapod	Racetrack	Triangle
Elongation	2.7	2.7	2.7	2.7	2.7
q_{95}	2.36	2.35	2.47	2.51	2.26
I_N , MA/mT	3.65	3.25	3.39	3.25	3.54
$\gamma_{n=0}$, s^{-1}	2504	1327	>10000	3080	>10000

assuming a constant elongation, κ=2.7, and constant beta, β_{tor}=1%. We note that the trapezoid (Fig.4B) is the only shape which has a lower n=0 growth rate than the classical D-shape. In addition, it was found that the current limit of the trapezoid increases with decreasing internal inductance. This property is important since the internal inductance can be varied by current profile tailoring, using ECRH [10].

Motivated by these theoretical results, we decided to test the trapezoidal shape experimentally. The creation of new plasma shapes is easy in TCV thanks to the MGAMS shape and position control algorithm [19]. MGAMS uses a preprogrammed evolution of the plasma shape and current to compute the poloidal field coil currents as functions of time. This implies the calculation of a number of free-boundary equilibria, using estimated values of poloidal beta and internal inductance. In Fig.5, we compare a trapezoidal plasma with a D-shaped plasma at the same elongation, κ=2.6 and the same beta value, β=1.1%. The D-shaped plasma

has a normalized current of I_N = 3.35 MA/mT, which is close to the limit, as seen in Fig.6. In these experiments, the current limit manifests itself by the appearance of MHD modes, with toroidal mode numbers, n>0, and subsequent disruptions [11]. In the trapezoidal scenario, we also pushed the current as high as possible, and we reached a maximum normalized current of I_N = 2.77 MA/mT. Open loop growth rates, as computed on the basis of the reconstructed experimental equilibria shown in Fig.5, are γ=2730 s^{-1} and γ=2118 s^{-1}, for the D-shaped and trapezoidal plasmas, respectively. These results are consistent with the theoretical results presented in Table 1, showing that the trapezoid has a lower current limit and a lower n=0 growth rate than the D-shape, at the same elongation. Attempts to extend the trapezoid scenario to higher elongations were unsuccessful, so far, due to the appearance of locked modes and subsequent disruptions. However, it is conceivable that the trapezoid will eventually reach higher elongation than the D-shape.

4. Limits to the operating space

4.1. Normalized current

Figure 6 shows the normalized current, $I_N=I_P/(a\,B)$, as a function of elongation. The upper limit of I_N increases dramatically with κ and, at the highest elongation, κ=2.8, the maximum normalized current is 4.5 times larger than at κ=1. The extension of the operating space obtained with the new, optimized vertical position control system consists of all data points with κ>2.58 and/or I_N >3.05 MA/mT. For κ<2.3, the current limit is approximately given by q_{95}=2, as seen in Fig.7. For κ>2.3, however, operation at q_{95}=2 is not possible and the minimum q-value increases with κ (Fig.7). This increase is consistent with ideal MHD stability calculations, as we shall see in section 4.4, where we compare theoretical and experimental current limits for a plasma with κ=2.5. There is also a lower limit to the normalized current, imposed by the axisymmetric mode. In Ohmic plasmas, both the internal inductance and the n=0 growth rate increase with decreasing current, and the minimum current is reached when the n=0 stability margin approaches zero. This lower limit depends on the current profile and can be influenced by profile tailoring, using electron cyclotron resonance heating (ECRH) or current drive (ECCD) [10]. The extension of the operating space due to this technique is seen in Figs. 6 and 7, where the red data points represent experiments with ECRH. It should be noted that these results are somewhat preliminary since, due to lack of experimental time, no attempt has yet been made to reach high elongation with ECRH at normalized currents I_N>1.

4.2. Greenwald fraction

Although we have not made a systematic effort to reach the maximum density for all possible shapes and elongations in TCV, it is nevertheless interesting to plot the Greenwald fraction, i.e. the line averaged density divided by the Greenwald density, n_G [20], as a function of elongation (Fig.8). Very high densities are usually achieved in TCV in ELM-free H-mode. However, this mode is only accessible for a limited set of plasma parameters [21]. In particular, at very high elongation, ELM-free H-modes cannot be produced in TCV because they require a divertor configuration, with a minimum plasma-wall distance of the order of 1cm, and these configurations are beyond the ideal n=0 stability limit. The striking decrease of the maximum Greenwald fraction with elongation can be explained by the fact that, in highly elongated, Ohmic plasmas, $\kappa>2.3$, the density limit coincides with the beta limit [11], and the beta limit is typically reached at Greenwald fractions between 10% and 30%. The results presented in Fig.8 do not imply that the density limit decreases with elongation. If we consider elongations in the range $1<\kappa<1.9$, we find that the density limit is approximately constant, since the maximum Greenwald fraction decreases by about the same factor as the maximum current increases (Fig.6). This is in agreement with results from DIII-D [22].

4.3. Axisymmetric stability margin

Using reconstructed experimental equilibria, we have calculated the stability margin of a subset of time slices in the TCV data base, covering mainly elongations $\kappa>2.2$ and triangularities $0.3<\delta<0.6$. The stability margin is defined here as $m_s=1/(\gamma\,\tau_V)$, where γ is the open-loop growth rate of the axisymmetric mode and τ_V is the decay time of the stabilizing currents in the vacuum vessel. Since, in the present context, we are mainly interested in general trends, rather than ultimate accuracy, we calculate the open loop growth rates with the Rigid Plasma Model (RPM), which is much less time consuming than the DPM [14]. This is justified by the fact that, within the parameter ranges considered here, the differences between RPM and DPM growth rates are small [14]. In Fig.9, we plot the stability margin as a function of elongation and we note that the maximum margin drops rapidly with elongation. The minimum stability margin, corresponding to the ideal n=0 stability limit, is theoretically given by $m_s=0$. In practice however, the margin must be slightly positive to allow for small pertubations such as sawteeth and ELMs. In TCV, the minimum stability margin is approximately $m_s=0.03$. In DIII-D, the achievement of $m_s=0.02$ has been reported [4]. Large tokamaks operate at much higher

stability margins. Typical values for JET and ITER-FEAT are $m_s>0.3$ and $m_s\sim0.5$, respectively.

4.4. Beta limit

The ideal MHD beta limit, as given by the n=1 external kink, for a D-shaped plasma in TCV with Ohmic current profile and $\kappa=2.5$ is shown in Fig.10 as a function of the normalized current. The typical uncertainty of the theoretical stability limit, as a result of small variations in the pressure and current profiles, within experimental error, is shown by an upper and a lower estimate (two blue lines in Fig.10). On the same figure, we plot experimental results representing virtually all TCV discharges with $\kappa<2.5$. We note that the experiments are entirely consistent with the theoretical predictions. In particular, experimental and theoretical current limits agree very well. The beta limit has been reached at very low and very high values of the normalized current. At intermediate values of I_N, however, where the beta limit is highest, the experimental data points are still far from the theoretical limit. There are two reasons for this. First, Ohmic plasmas with $\kappa=2.5$ and $I_N\sim2$ cannot be created in TCV since they are ideally unstable with respect to the axisymmetric mode and cannot be stabilized by any feedback system no matter how fast it is. Such plasmas can only be stabilized by broadening the current profile, using off-axis ECRH, but up to now this technique has only been tried at low current, $I_N<0.8$ MA/mT [10]. The second reason for the discrepancy between experimental and theoretical stability limits is that the main heating system on TCV, i.e. 2nd harmonic ECRH, can only be used at low density [23], and under these conditions it is impossible to reach high beta. In Fig. 11, we plot the normalized beta, $\beta_N=\beta_{tor}/I_N$, as a function of the safety factor, q_{95}, for all TCV discharges, irrespective of elongation. Ohmic and ECRH experiments are shown in green and red, respectively. It should be pointed out, however, that the results presented here do not represent the ultimate capabilities of TCV. A 3rd harmonic ECRH system has recently been installed on TCV [24] and this will allow us to heat plasmas at higher density and to reach higher beta-values.

5. Conclusions

The TCV operating space was previously limited to $\kappa<2.58$ and $I_N<3.05$ [12] due to a non-optimal vertical position control system and the presence of a toroidal belt limiter, which restricted the plasma minor radius. The operating space has recently been extended to $\kappa<2.80$ and $I_N<3.60$, as a result of a systematic optimization of the vertical feedback system and of the

plasma shape. Extensive DPM calculations have been performed in order to optimize the vertical position observer, the transfer function of the feedback control loop and the configuration of active coils. This has allowed us to operate much closer to the natural plasma limits than was previously posssible. MHD stability properties of a large number of theoretical free-boundary equilibria have been computed with the aim of optimizing the plasma shape. It was found that, for a given elongation, κ=2.7, the n=0 growth rate at the n=1 current limit has a minimum in the (δ, λ) plane and that the values of δ and λ at the minimum are in good agreement with optimum experimental conditions for reaching high elongation. Finally, we have shown that the experimental current and beta limits are consistent with ideal MHD stability calculations, using measured plasma shapes and profiles.

Acknowledgements

It is a pleasure to acknowledge the competent support of the entire TCV team. This work was partly supported by the Fonds National Suisse de la Recherche Scientifique.

References

[1] Lomas, P.J. et al., Plasma Phys. Control. Fusion **42** (2000) B115.

[2] Cordey, J.G. et al., Plasma Phys. Control. Fusion **39** (1997) B115.

[3] Kamada, Y. et al., in Fusion Energy 1996 (Proc. 16th Int. Conf. Montreal, 1996), Vol. 1, IAEA, Vienna (1997) 247.

[4] Lazarus, E.A. et al., Phys. Fluids **B4** (1992) 3644.

[5] Troyon, F. et al., Plasma Phys. Control. Fusion **26** (1984) 209.

[6] Phillips, M.W. et al., in Plasma Physics and Controlled Nuclear Fusion Research 1988 (Proc. 12th Int. Conf. Nice, 1988), Vol. II, IAEA, Vienna (1989) 65.

[7] Turnbull, A.D. et al., Nucl. Fusion **28** (1988) 1379.

[8] Eriksson, G. et al., in 1992 International Conference on Plasma Physics (Proc. Conf. Innsbruck 1992), Vol. 16C, Part I, European Physical Society, Geneva (1992) I-343.

[9] Menard, J.E. et al., Nucl. Fusion **37** (1997) 595.

[10] Pochelon, A. et al., Nucl. Fusion **41** (2001) 1663

[11] Hofmann, F. et al., Phys. Rev. Lett. **81** (1998) 2918.

[12] Hofmann, F. et al., Nucl. Fusion **38** (1998) 399.

[13] Lazarus, E.A., et al., Nucl. Fusion **30** (1990) 111.

[14] Hofmann, F. et al., Nucl. Fusion **38** (1998) 1767.

[15] Hofmann, F. et al., Nucl. Fusion **40** (2000) 767.

[16] Lister, J.B. et al., Fusion Technology **32** (1997) 321.

[17] Lister, J.B. et al., Nucl. Fusion **36** (1996) 1547.

[18] Degtyarev, L. et al., Comput. Phys. Commun. **103** (1997) 10.

[19] Hofmann, F. et al., in Controlled Fusion and Plasma Physics (Proc. 22nd Eur. Conf. Bournemouth, 1995), Vol. 19C, Part II, European Physical Society, Geneva (1995) 101.

[20] Greenwald, M. et al., Nucl. Fusion **28** (1988) 2199.

[21] Martin, Y. et al., in Fusion Energy 2000 (Proc. 18th Int. Conf. Sorrento 2000), to be published in Nucl. Fusion.

[22] Petrie, T.W., et al., Nucl. Fusion **33** (1993) 929.

[23] Coda, S. et al., Plasma Phys. Control. Fusion **42** (2000) B311.

[24] Alberti, S. et al., Proc. 18th IAEA Fusion Energy Conf., Sorrento 2000, papper PD/2, accepted for publication in Nucl. Fusion.

Figure Captions

Fig.1 DPM predictions of stability limits of the TCV vertical position control system, in three-dimensional gain space, under closed-loop conditions, for a D-shaped plasma with I_P=351kA, B_{tor}=1.0T, κ=2.11, δ=0.42, $\gamma_{n=0}$=2300 s^{-1}.

Fig.2 Poloidal cross-section of the TCV tokamak, showing the OH transformer (A1, B1, B2, C1, C2, D1, D2), shaping coils (E1-E8, F1-F8), internal coils for vertical position control (G1, G2), magnetic probes (1-38) and flux surfaces of an experimental plasma with I_P=750kA, B_{tor}=0.8T, κ=2.80, δ=0.53, $\gamma_{n=0}$=2623 s^{-1} (TCV shot 19373).

Fig.3 (A) Ideal MHD current limit, in kA, due to n=1 mode and (B) n=0 growh rate in s^{-1} at the current limit, as a function of the shape parameters (δ and λ), for D-shaped plasmas with κ=2.7.

Fig.4 Theoretical TCV equilibria of various shapes: (A): classical D-shape, (B): trapezoid, (C): peapod, (D): racetrack, (E): triangle. Current and pressure profiles are taken from an experimental discharge with κ=2.7 (# 19034).

Fig.5 Comparison of D-shaped and trapezoidal plasmas in TCV. (A) D-shape, κ=2.60, I_N=3.35 MA/mT, β_{tor}=1.1%, $\gamma_{n=0}$=2730 s^{-1} (B) trapezoid, κ=2.61, I_N=2.77 MA/mT, β_{tor}=1.1%, $\gamma_{n=0}$=2118 s^{-1}.

Fig.6 Normalized current, $I_P/(a\,B)$ [MA/mT], vs. elongation for all TCV discharges between March 1994 and May 2001. Ohmic and ECRH experiments are shown in green and red, respectively.

Fig.7 Safety factor (q_{95}) vs. elongation for all TCV discharges between March 1994 and May 2001. Ohmic and ECRH experiments are shown in green and red, respectively. Ideal n=1 stability limit is shown by the solid blue line.

Fig.8 Greenwald fraction, $\langle n_e \rangle / n_{GW}$, vs elongation for all TCV discharges between March 1995 and May 2001.

Fig.9 Axisymmetric stability margin, $m_s=1/(\gamma\,\tau_V)$, vs. elongation, as obtained from RPM caculations, using reconstructed experimental equilibria.

Fig.10 Toroidal beta, as obtained from LIUQE equlibrium reconstructions, vs. normalized current, for all TCV discharges between March 1994 and May 2001 with κ<2.5. Ideal MHD stability limits for a D-shaped, Ohmic plasma with κ=2.5 are shown in blue. Ohmic and ECRH experiments are shown in green and red, respectively.

Fig.11 Normalized beta vs. q_{95}, for all TCV discharges between March 1994 and May 2001. Ohmic and ECRH experiments are shown in green and red, respectively.

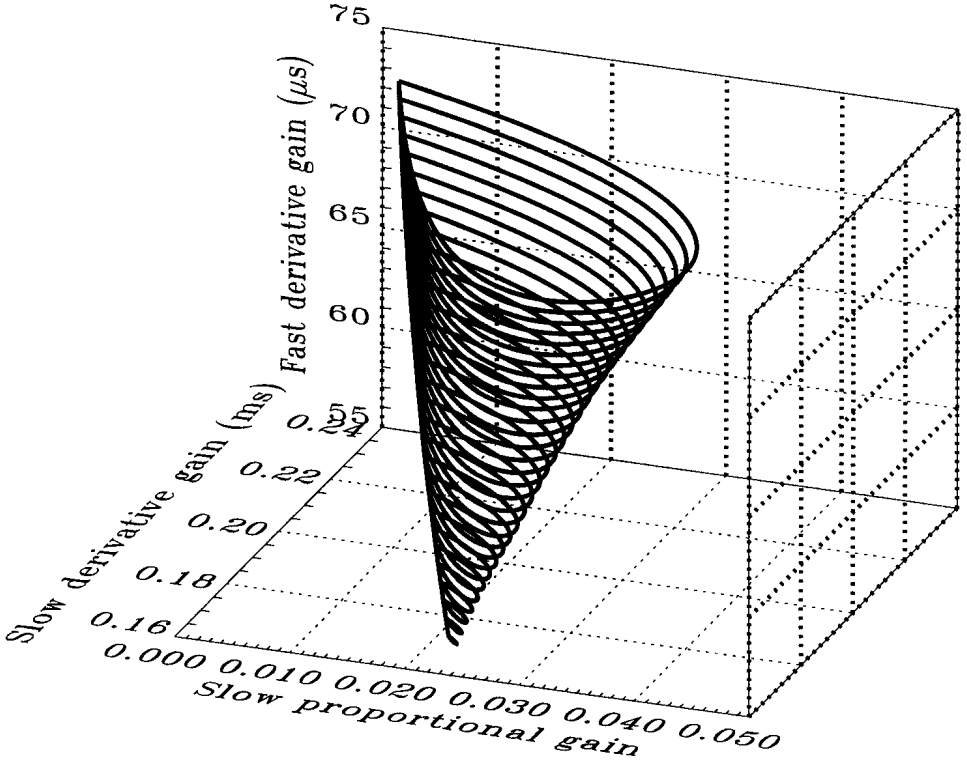
75
70
65
60
55
Fast derivative gain (μs)
0.24
0.22
0.20
0.18
0.16
Slow derivative gain (ms)
0.000 0.010 0.020 0.030 0.040 0.050
Slow proportional gain

Fig. 1

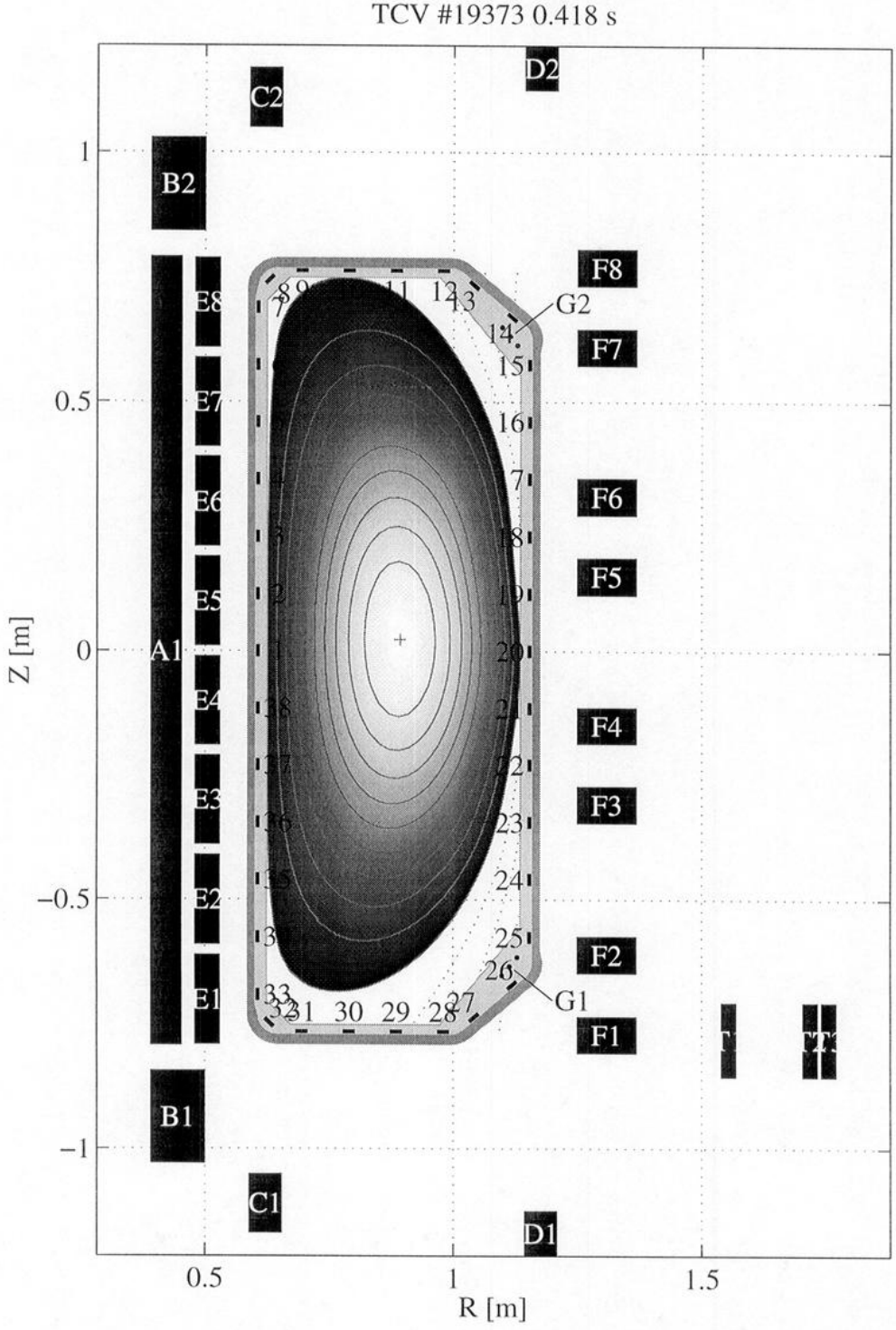
TCV #19373 0.418 s
D2
C2
B2
F8
G2
F7
E8
E7
E6
E5
E4
E3
E2
E1
A1
F6
F5
F4
F3
F2
F1
G1
B1
C1
D1
Z [m]
R [m]
1
0.5
0
−0.5
−1
0.5
1
1.5

Fig. 2

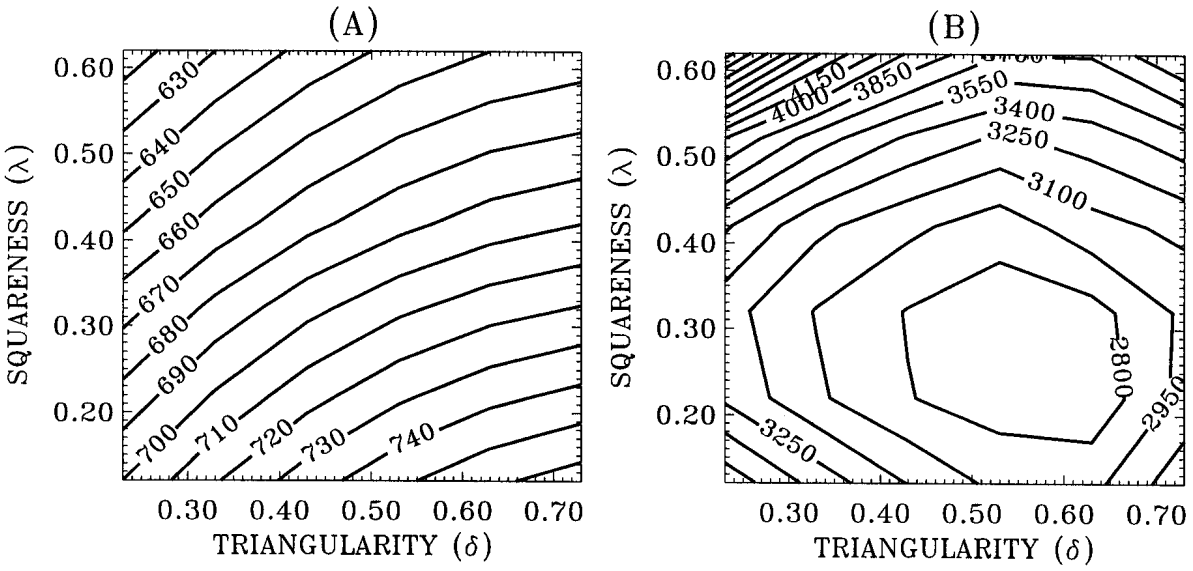
(A)
(B)
SQUARENESS (λ)
TRIANGULARITY (δ)
0.60
0.50
0.40
0.30
0.20
0.30 0.40 0.50 0.60 0.70
630
640
650
660
670
680
690
700
710
720
730
740
4150
4000
3850
3550
3400
3250
3100
2800
2950
3250

Fig. 3

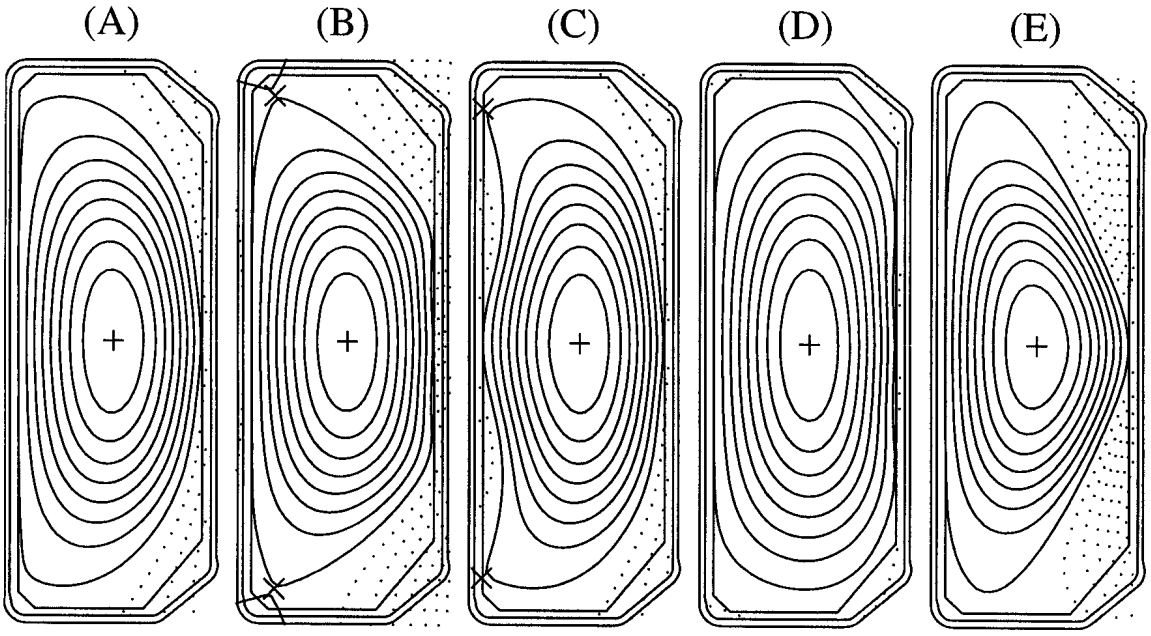

Fig. 4

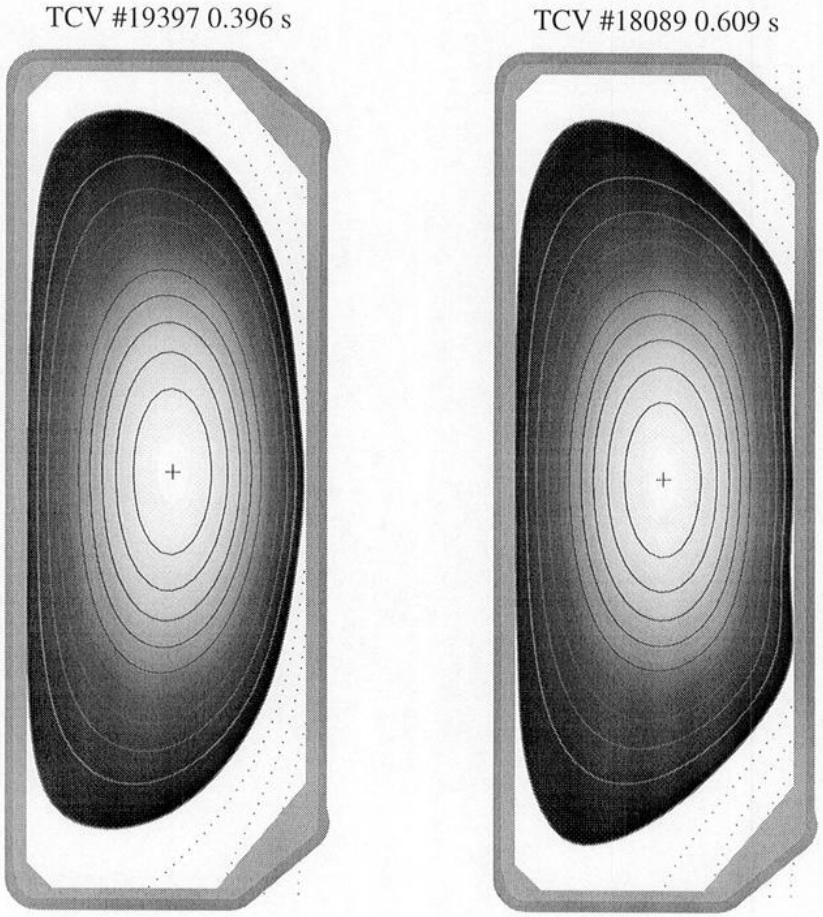

Fig. 5

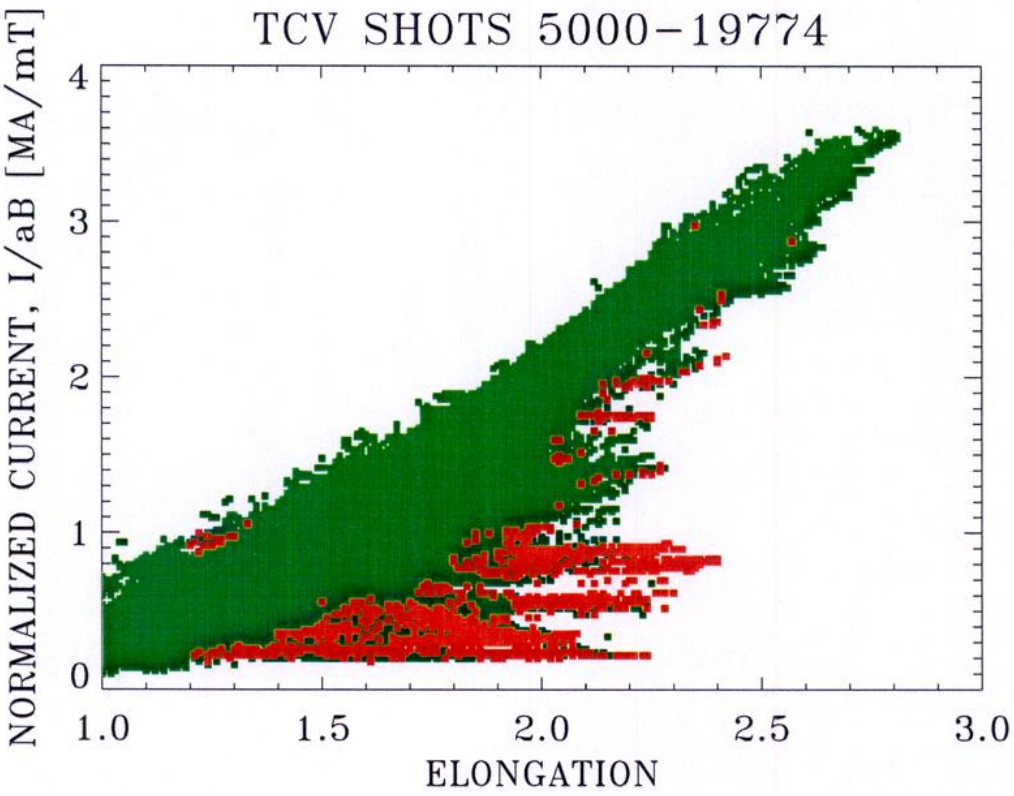
TCV SHOTS 5000−19774
NORMALIZED CURRENT, I/aB [MA/mT]
0
1
2
3
4
1.0
1.5
2.0
2.5
3.0
ELONGATION

Fig. 6

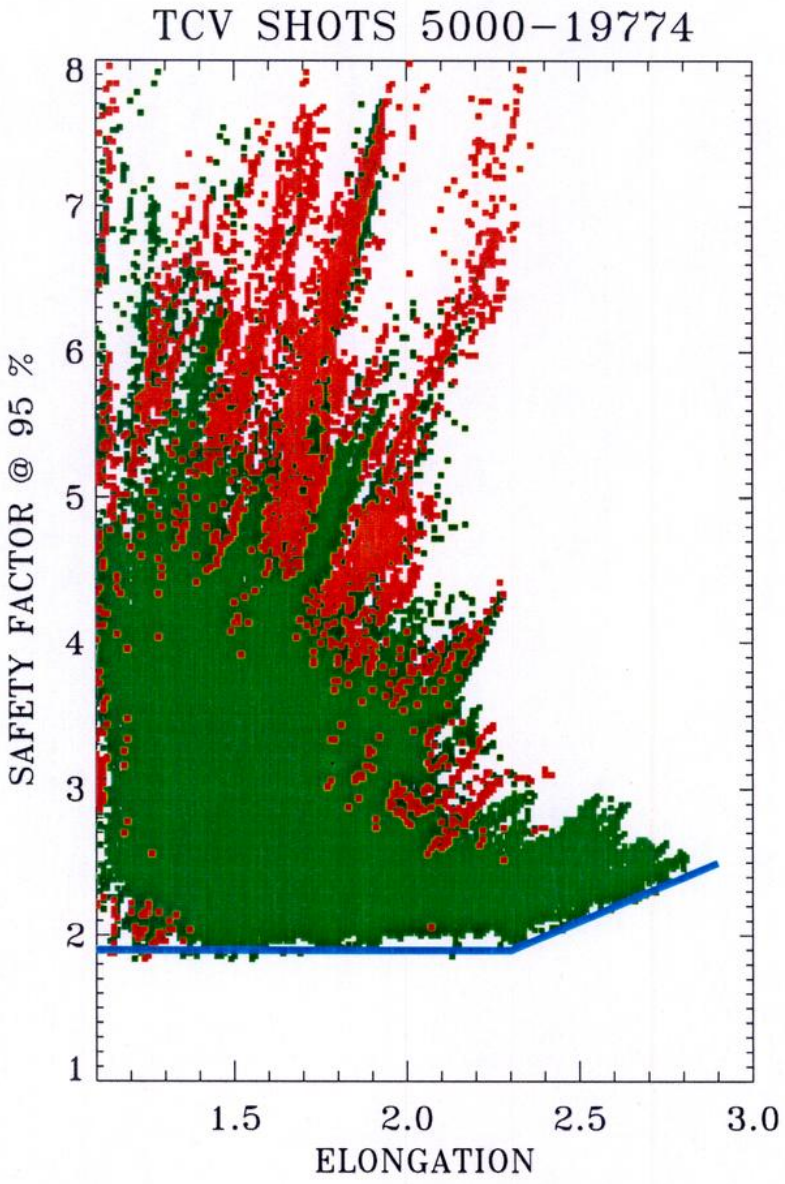
TCV SHOTS 5000−19774
SAFETY FACTOR @ 95 %
ELONGATION
1
2
3
4
5
6
7
8
1.5
2.0
2.5
3.0

Fig. 7

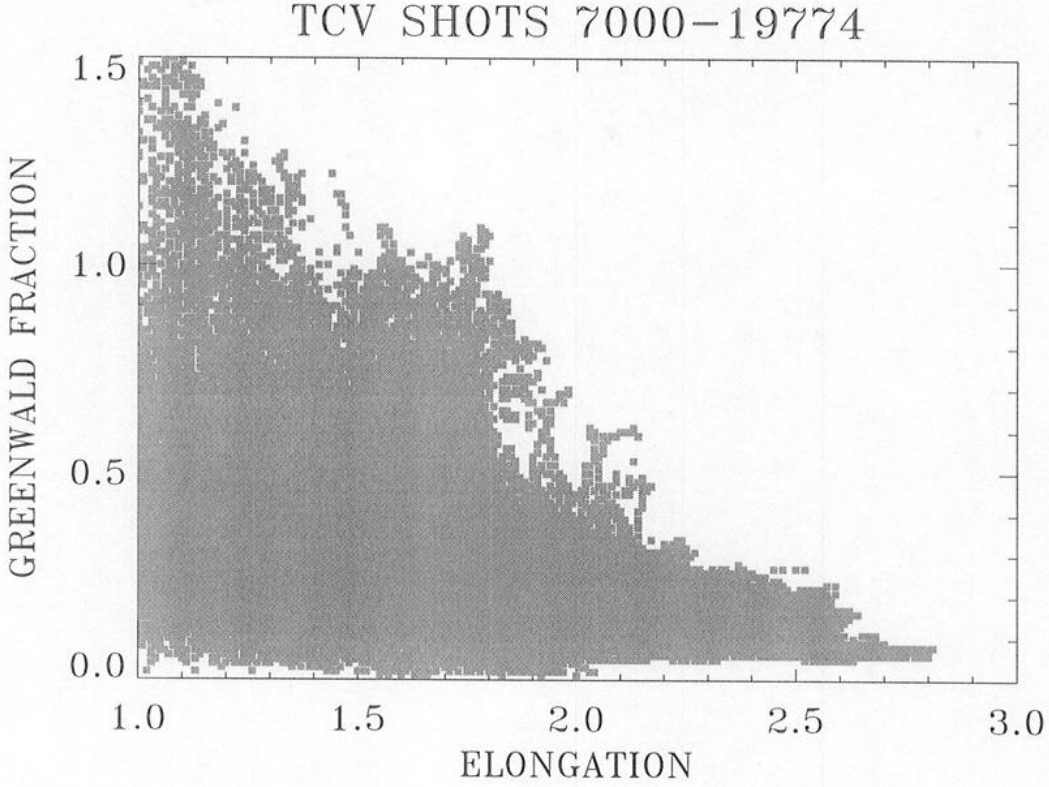
TCV SHOTS 7000-19774
GREENWALD FRACTION
1.5
1.0
0.5
0.0
1.0
1.5
2.0
2.5
3.0
ELONGATION

Fig. 8

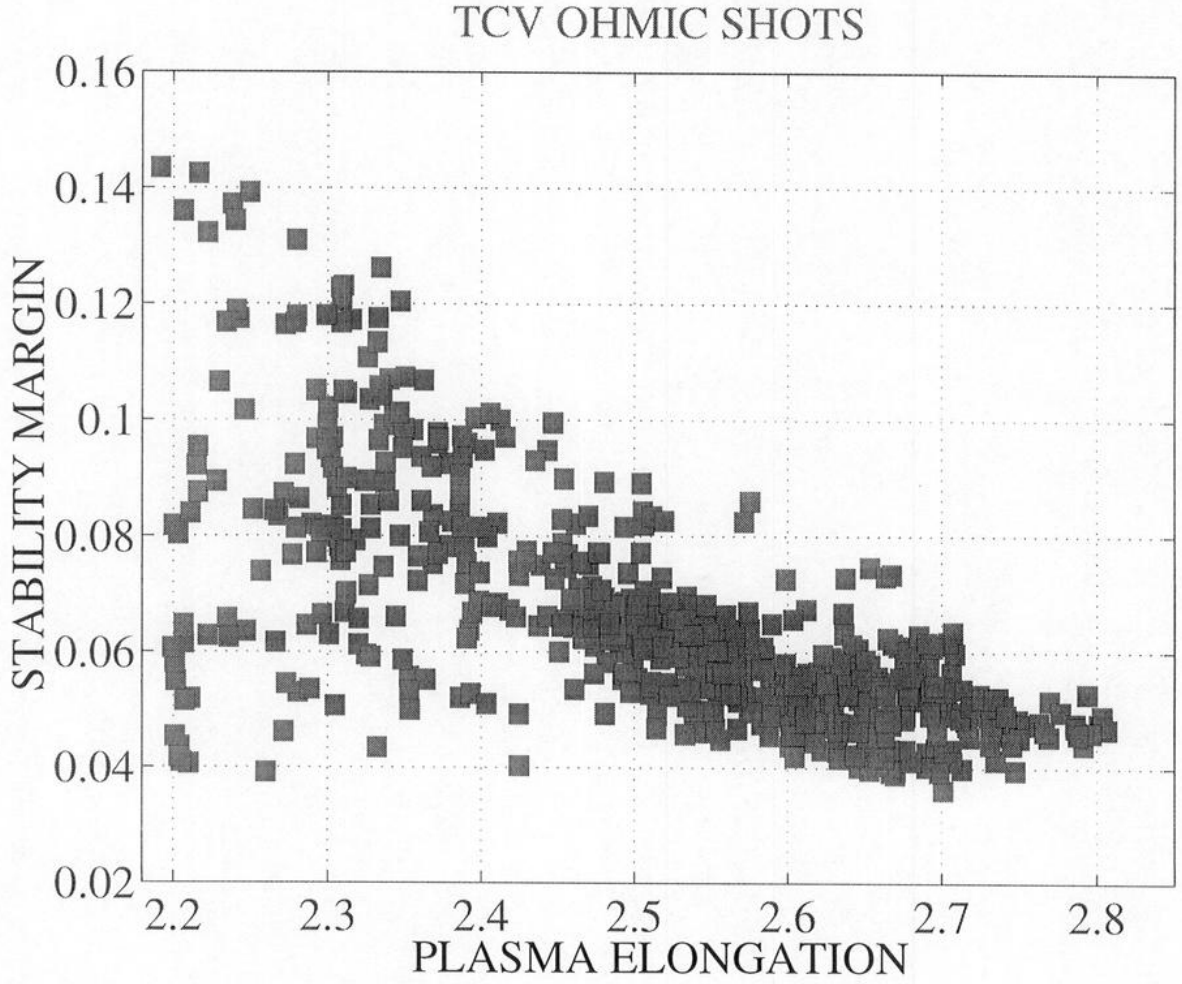
TCV OHMIC SHOTS
STABILITY MARGIN
0.16
0.14
0.12
0.1
0.08
0.06
0.04
0.02
2.2
2.3
2.4
2.5
2.6
2.7
2.8
PLASMA ELONGATION

Fig. 9

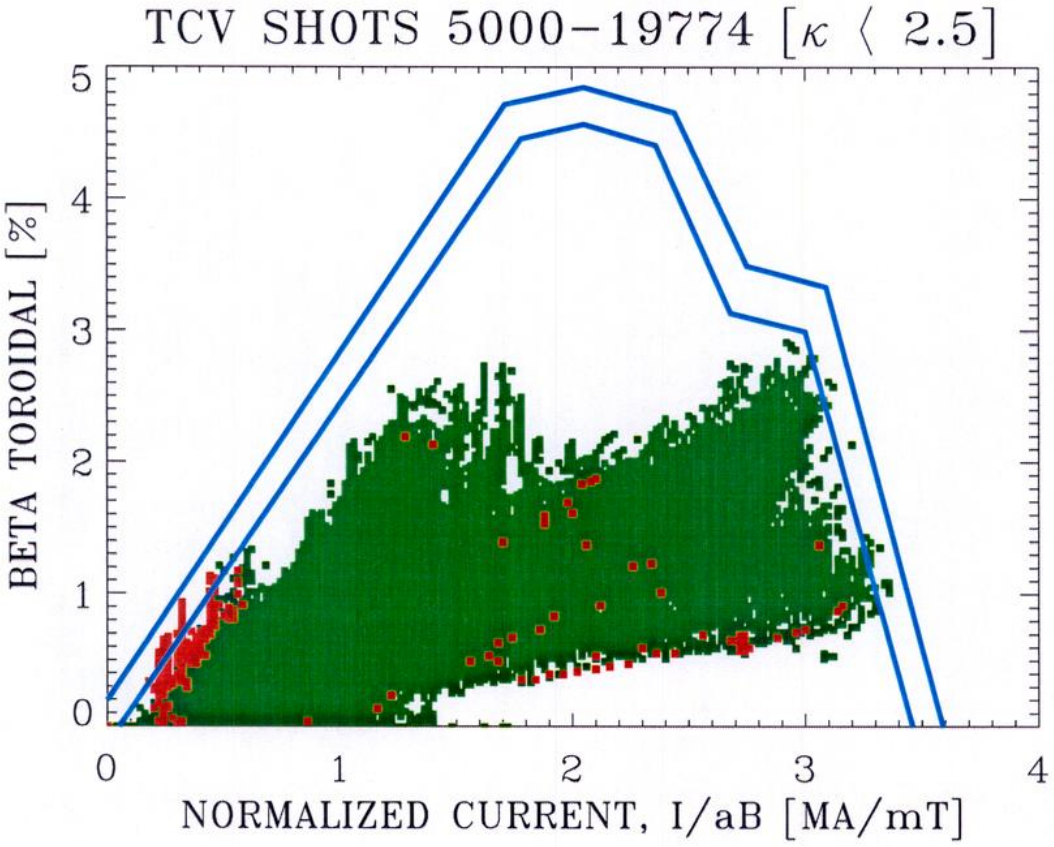
TCV SHOTS 5000−19774 [κ ⟨ 2.5]
BETA TOROIDAL [%]
0
1
2
3
4
5
0
1
2
3
4
NORMALIZED CURRENT, I/aB [MA/mT]

Fig. 10

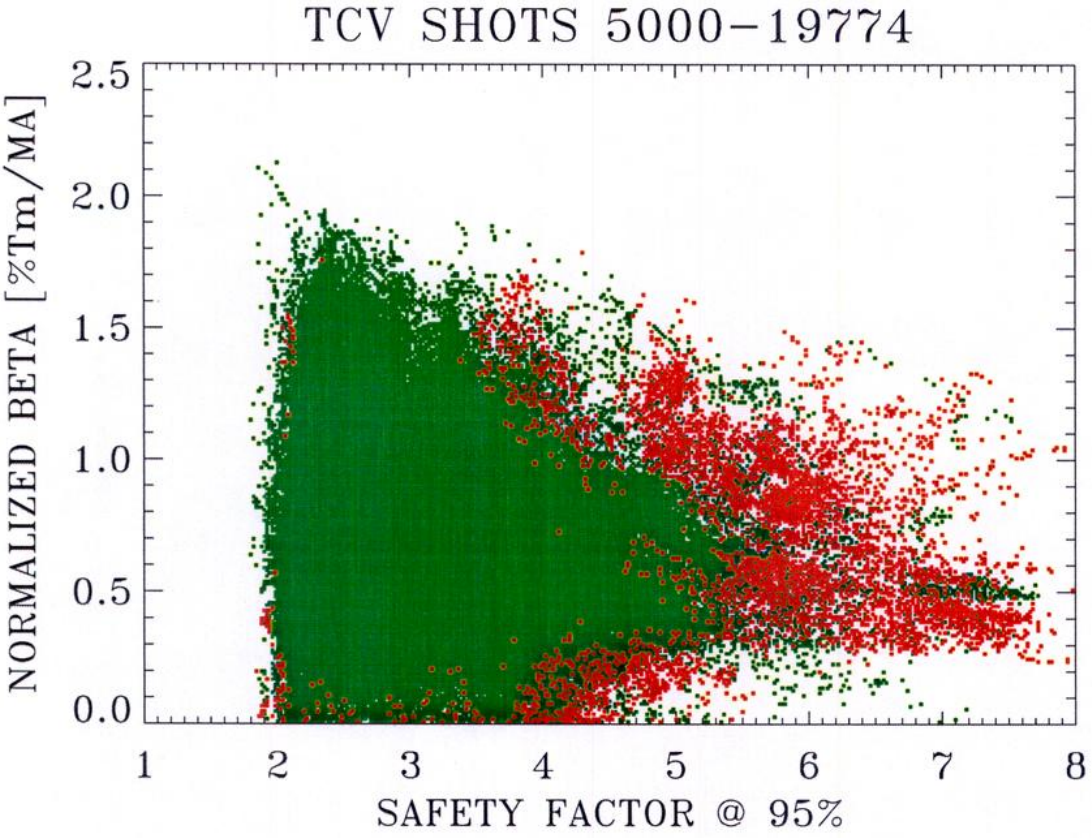
TCV SHOTS 5000-19774
NORMALIZED BETA [%Tm/MA]
2.5
2.0
1.5
1.0
0.5
0.0
1
2
3
4
5
6
7
8
SAFETY FACTOR @ 95%

Fig. 11